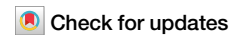


<https://doi.org/10.1038/s43247-025-02410-1>

# Subduction transference drove the Mesozoic convergence of microcontinents from Gondwana to Asia

Yiming Ma<sup>1,2</sup>✉, Mark J. Dekkers<sup>3</sup>, João C. Duarte<sup>3</sup> & Timothy Kusky<sup>4</sup>

How microcontinents successively migrated from Gondwana to Eurasia is paramount in understanding the Mesozoic evolution of the Tethys Ocean. The rifting and collision events and their potential spatio-temporal relationship may play a key role in this evolution. We compiled available Permian–Jurassic paleomagnetic data from the Lhasa terrane, revealing that it drifted away from Gondwana ~210 million years ago, which is ~10 million years earlier than the South–North Qiangtang collision. Similarly, the Lhasa–Qiangtang collision preceded the rifting of India by ~10 million years. These age gaps of similar kinematic circuits align well with the time required for collision-induced subduction transference, whereby a new subduction zone forms outboard of the newly accreted terrane. Then, the slab-pull force can be transmitted to the southern segment of the younger Tethys slab by coupling across the oceanic ridge/transform system, such that subduction transference drives the in-sequence one-way convergence of microcontinents with Eurasia.

In plate tectonics, plate convergence starts with subduction initiation and stops or slows considerably when continents collide. The slab-pull force caused by oceanic slab subduction is regarded as a critical driver of plate motion<sup>1,2</sup>. This concept is also considered a foremost explanation for the breakup of microcontinents from Gondwana and their successive accretion onto Asia<sup>3,4</sup>. In the so-called one-way accretion onto Asia, each terrane moved northward from Gondwana, driven by the slab-pull force due to the subduction of the oceanic slab, until it collided with Asia. Afterwards, the northward subduction of the next oceanic slab south of the just-accreted terrane is resumed to accommodate the continuous convergence, forming a new subduction zone. This process is called collision-induced subduction transference<sup>5,6</sup>. Subduction transference here means the subduction is transferred from an older Tethys oceanic crust to a younger ocean on the back side of the accreted terrane, cf. Yang<sup>5</sup>. Notably, coupling across the oceanic ridge/transform system in the younger ocean enables the slab-pull force to be transmitted to the northern margin of Gondwana. Therefore, collision-induced subduction transference may be critical to explaining a unique feature of Tethyan evolution, i.e., the one-way (northward) convergence of a series of microcontinents from Gondwana to Asia, one after the other.

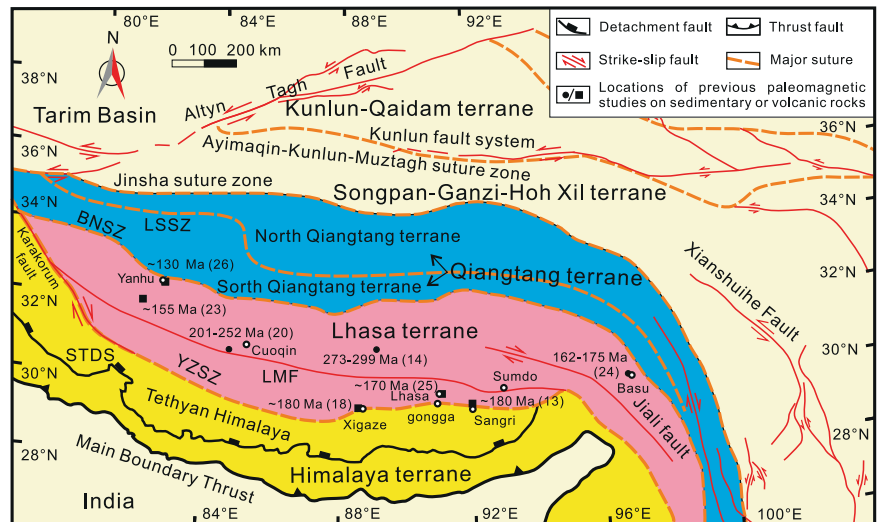
However, the potential spatio-temporal relationship between subduction transference and the plate motion cycle of unidirectional

convergence remains unclear, if it exists at all. Numerical modeling has shown that the subduction initiation associated with collision-induced subduction transference generally occurs within ~10 million years (Myr) after a collision<sup>6</sup>. This means that if the rifting of the microcontinents from Gondwana were caused directly by subduction transference, their rifting should postdate the collision of the previous terrane with Asia by ~10 Myr. To verify this potential spatio-temporal relationship, one should first precisely constrain the kinematics, particularly the timing of the rifting and collision. The Tibetan Plateau results from the one-way northward convergence of microcontinents originating from Gondwana<sup>7,8</sup>; it is an unparalleled natural laboratory to constrain these kinematic scenarios. The plateau consists of the Qiangtang, Lhasa, and Himalaya terranes, separated respectively by the Bangong–Nujiang suture zone (BNSZ or Meso–Tethys) and the Yarlung–Zangpo suture zone (YZSZ or Ceno–Tethys) (Fig. 1). The terranes accreted onto the southern margin of mainland Asia in the Late Triassic<sup>8,9</sup>, Late Jurassic–Early Cretaceous<sup>10</sup> and Paleocene–Eocene<sup>11</sup>, respectively, closing the Paleo-, Meso-, and Ceno-Tethys Oceans one by one<sup>7</sup>. The kinematic history of the Lhasa terrane, sandwiched between the Qiangtang and Himalaya terranes by two Tethys suture zones, is thus central to the concept of one-way convergence of these terranes.

Notably, when the Lhasa terrane rifted from the northern margin of Gondwana has remained controversial for about four decades<sup>12</sup>. Estimates

<sup>1</sup>School of Earth Sciences, China University of Geosciences, Wuhan, Wuhan, China. <sup>2</sup>Department of Earth Sciences, Paleomagnetic Laboratory “Fort Hoofddijk”, Utrecht University, Utrecht, The Netherlands. <sup>3</sup>Instituto Dom Luiz (IDL) and Geology Department, Faculty of Sciences, University of Lisbon, Lisbon, Portugal. <sup>4</sup>State Key Laboratory of Geological Processes and Mineral Resources, Center for Global Tectonics, School of Earth Sciences, China University of Geosciences, Wuhan, Wuhan, China. ✉e-mail: [may.iming2006@163.com](mailto:may.iming2006@163.com)

**Fig. 1** | Geologic map of the Tibetan Plateau and adjacent areas (modified from Yin<sup>8</sup>). Indicated are the major terranes and suture zones on the Tibetan Plateau. Abbreviations: BNSZ, Bangong-Nujiang suture zone separating the Qiangtang and Lhasa terranes; LMF, Luobadui-Milashan fault, which divides the Lhasa terrane into northern and southern parts; LSSZ, Longmuco-Shuanghu suture zone, which divides the Qiangtang terrane into the North and South Qiangtang terranes; STDS, South Tibet detachment system, which separates the Tethyan Himalaya from other parts of the Himalaya terrane; YZSZ, Yarlung Zangbo suture zone, which separates the Lhasa terrane from the Himalaya terrane. Numbers (in Ma) indicate the rock ages in relevant Permian-Jurassic paleomagnetic studies<sup>13,14,18,20,23–26</sup>. On the map, cyan, magenta, and yellow denote the Qiangtang, Lhasa, and Himalaya terranes, respectively, while light yellow represents other blocks.



range widely from earlier than the Permian to the Late Triassic based on paleontologic, geologic, and geophysical data<sup>13–16</sup>. For example, some authors suggested that Lhasa drifted away from the Indian segment of Gondwana together with the Qiangtang terrane based on lower Permian mafic volcanic rocks and middle Permian overlying sedimentary strata<sup>16</sup>. In contrast, other research teams suggested that the Lhasa terrane rifted from Australia in the Late Triassic based on age spectra and trace element chemistry of detrital zircons<sup>17</sup>. However, both scenarios lack robust evidence on the drift history of the Lhasa terrane to constrain when and where it rifted from Gondwana.

The Lhasa terrane moved northward while India-Australia was moving southward during the Jurassic<sup>13,18,19</sup>, indicating a spreading ridge (with a transform fault system) between them in this period. Therefore, the drift history of the Lhasa terrane during the Triassic-Jurassic is critical in understanding its breakup from eastern Gondwana<sup>13,18,20</sup>. Here, we review available paleomagnetic data from the Tibetan plateau, especially from the Lhasa terrane, combined with evidence from geology and geophysics, to strive to answer the following issues: (1) When did Lhasa rift from Gondwana? (2) Is there a potential spatiotemporal relationship between the collision and rifting events? (3) What are the dynamic implications of subduction transference and the plate motion cycle of unidirectional convergence?

## Paleolatitude evolution of the Lhasa terrane during Permian to Jurassic

Reliable Mesozoic paleomagnetic data used for paleogeographic reconstruction should rely on field tests to ensure a primary natural remanent magnetization (NRM) and on enough input records to average out paleosecular variation. We suggest reliable paleomagnetic results should fulfill the following criteria based on Van der Voo<sup>21</sup> and Meert et al.<sup>22</sup>, which have been widely used in paleomagnetic investigations. (1) Well-determined rock age with magnetization deemed of the same age; (2) effective demagnetization and statistical analysis with  $N \geq 25$  samples for sedimentary rocks or  $B \geq 8$  sites for volcanic sites; (3) reliable rock-magnetic support; (4) field tests that demonstrate the age of the magnetization; (5) reliable structural control; and (6) no resemblance to younger poles.

Based on our data selection criteria, some previous paleomagnetic results<sup>14,20</sup> from sedimentary rocks are considered questionable: their paleopoles of Permian<sup>14</sup> and Early-Middle Triassic<sup>20</sup> age are similar to that of the Late Triassic<sup>20</sup>, violating criterion (6); presumably, those rocks are remagnetized. In contrast, the Late Triassic paleopole<sup>20</sup> differs from younger poles. Its positive fold test suggests a primary origin. Consequently, there is no reason to exclude it from further discussion. Thus, six pre-Cretaceous

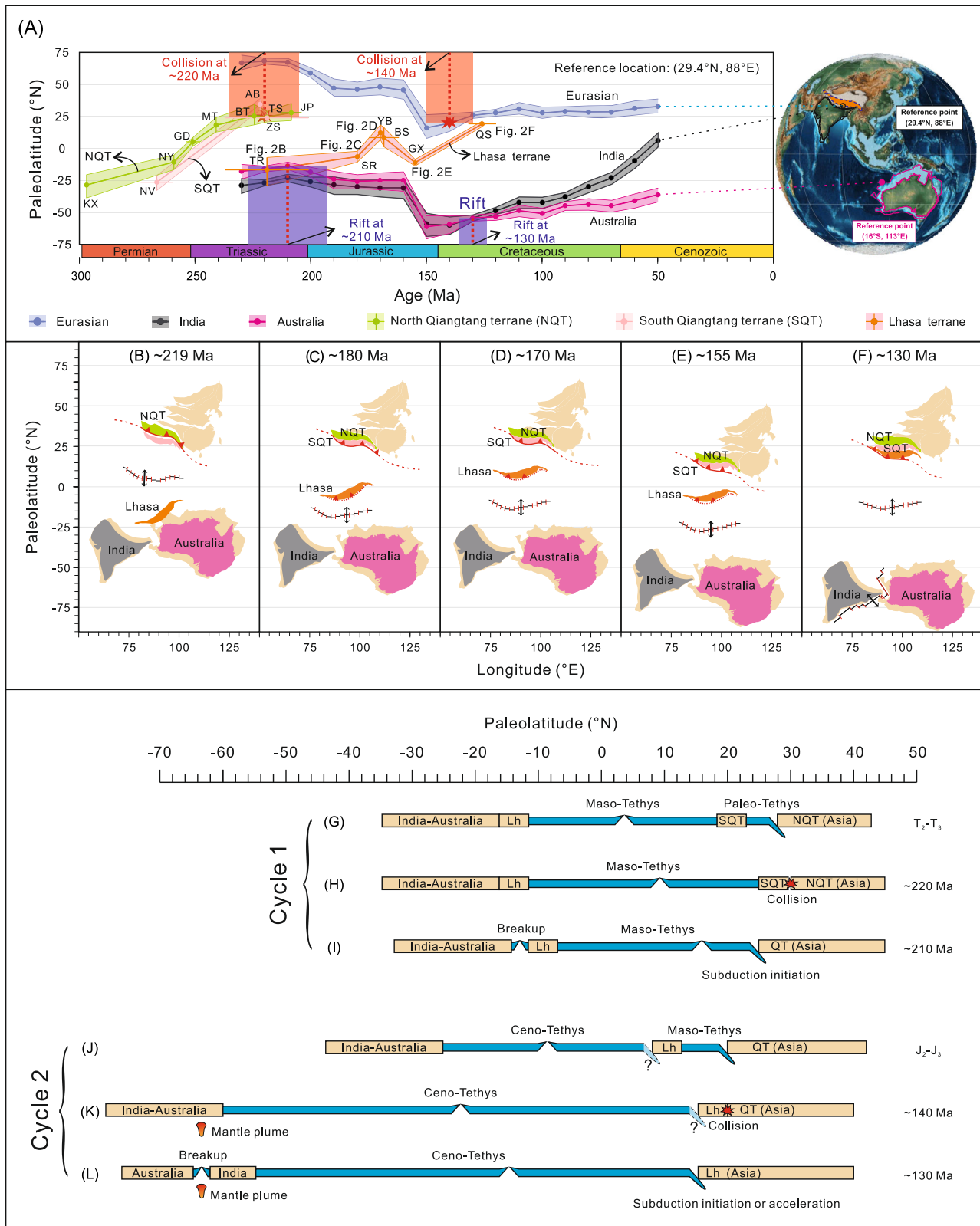
paleomagnetic results<sup>13,18,20,23–25</sup> are deemed reliable and used to constrain the paleolatitude of the Lhasa terrane at the reference point (29.4°N, 88°E) at the central part of the YZSZ (Fig. 2A–E) (Supplementary Table 1). The Late Triassic paleomagnetic results of six sedimentary sites (37 specimens) from the Cogen area, passing a fold test (95% confidence level), position the Lhasa terrane at  $17.0^\circ \pm 10.7^\circ\text{S}$  at  $\sim 219$  million years ago (Ma)<sup>20</sup> (Fig. 2B). The Early Jurassic paleomagnetic results with positive fold and reversal tests reported by Li et al.<sup>13</sup> and Ma et al.<sup>18</sup> yield a paleolatitude of  $6.6^\circ \pm 4.2^\circ\text{S}$  at  $\sim 180$  Ma (Fig. 2C). For the Middle Jurassic ( $\sim 170$  Ma), Otofujii et al.<sup>24</sup> and Wang et al.<sup>25</sup> reported paleopoles based on sedimentary and volcanic rocks, respectively, yielding a paleolatitude of  $\sim 8$ – $12^\circ\text{N}$  for the Lhasa terrane (Fig. 2D). Li et al.<sup>23</sup> presented a new paleomagnetic pole from the Zenong Group volcanics in the Geji area, corresponding to a paleolatitude of  $11.3^\circ \pm 2.5^\circ\text{S}$  at  $\sim 155$  Ma (Fig. 2E).

Based on reliable paleolatitudes of  $17.0^\circ \pm 10.7^\circ\text{S}$  at  $\sim 219$  Ma,  $6.6^\circ \pm 4.2^\circ\text{S}$  at  $\sim 180$  Ma,  $\sim 8$ – $12^\circ\text{N}$  at  $\sim 170$  Ma,  $11.3^\circ \pm 2.5^\circ\text{S}$  at  $\sim 155$  Ma, and  $18.9^\circ \pm 2.1^\circ\text{N}$  at  $\sim 130$  Ma (Fig. 2A), Lhasa terrane's motion during  $\sim 219$ – $130$  Ma can be divided into three stages: (1) a northward drift from the southern to the northern hemisphere from  $\sim 219$  Ma to  $\sim 170$  Ma, leading to the separation of Lhasa and Australia; (2) an apparent fast southward movement from  $\sim 170$  Ma to  $\sim 155$  Ma due to Jurassic TPW<sup>18</sup>; (3) a northward approach to Eurasia and collision with the Qiangtang terrane in the Late Jurassic-Early Cretaceous ( $\sim 140$  Ma) in the northern hemisphere. The Lhasa terrane is situated at a stable paleolatitude after the Lhasa-Qiangtang collision; it has become the southern margin of Asia (awaiting the later India-Asia collision)<sup>26</sup>.

## Lhasa terrane rifted from Gondwana at $\sim 210 \pm 14$ Ma

The paleolatitude of  $17.0^\circ \pm 10.7^\circ\text{S}$  at  $\sim 219$  Ma, which is the only reliable pre-Jurassic paleopositional constraint, agrees well with the paleolatitude of northwestern Australia<sup>27,28</sup> and possibly Greater India, indicating that the Lhasa terrane was most likely connected to Australia and/or Greater India at this time (Fig. 2B).

The Ceno-Tethys opened when the Lhasa terrane rifted away from the northern margin of eastern Gondwana. Therefore, understanding the drift history of both entities is central to understanding the evolution of the Ceno-Tethys. A reference point (16°S, 113°E) in northwestern Australia was chosen to assess the paleolatitude evolution of eastern Gondwana for the following reasons: (1) the northern extension of Greater India remains controversial<sup>11</sup>, (2) India-Australia is a stable part of eastern Gondwana until  $\sim 130$  Ma upon their breakoff<sup>29</sup>, (3) India and Australia share a similar expected paleolatitude based on their apparent polar wander paths<sup>28</sup>, and (4) the Lhasa terrane may originate from northwestern Australia based on the



similarity of zircon age profiles from NW Australia and Lhasa<sup>17,30</sup>. The open-source environment Paleomagnetism.org was used to calculate the respective paleolatitudes<sup>27,28</sup>.

As shown in Fig. 2A, B, the expected paleolatitude of eastern Gondwana is ~16.3°S at 220 Ma for the reference point (16°S, 113°E), consistent with ~17.0°S at ~219 Ma of the Lhasa terrane for the reference point

(29.4°N, 88°E). These overlapping paleolatitudes suggest that Lhasa and Australia were close to each other at ~219 Ma. Even though some researchers suggest that a back-arc basin was present between Lhasa and Gondwana during the Late Triassic<sup>31</sup>, our updated paleolatitude evolution shows that this potential back-arc basin was small at ~219 Ma if it existed at all.

**Fig. 2 | Reconstruction of paleolatitude, paleogeography and kinematic cycles of the Lhasa terrane and adjacent blocks.** This figure shows the paleolatitude evolution (A) and paleo-position reconstruction (B–F) of the Lhasa terrane and adjacent blocks, including the two simplified kinematic cycles without ridge subduction (G–L). Two subduction transference events in cycle 1 (Fig. 2G–I) and cycle 2 (Fig. 2J–L) are identified in building Eurasia. The age uncertainty of the rifting events is based on paleolatitude evolution and geologic observations (see text for details). The possible southward subduction of the Meso-Tethys below Lhasa and its age remains controversial and, thus, is not indicated here to avoid confusion (See Supplementary Note 1). The exact locations of the mid-ocean ridges in the Meso-Tethys and Ceno-Tethys Oceans are somewhat uncertain; therefore, they are depicted near the centers of these oceans (Fig. 2B–F). The paleolatitude evolution is generated with [www.paleomagnetism.org](http://www.paleomagnetism.org)<sup>28</sup>. The observed paleolatitudes of the Lhasa, North Qiangtang, and South Qiangtang terranes are calculated from the data compiled in Supplementary Table 1. In our kinematic reconstruction, we observed a

rapid TPW event during the Late Jurassic period<sup>18</sup> (Fig. 2A). This event is supported by several paleomagnetic data collected from continental and oceanic plates<sup>68,69</sup>. The Late Jurassic–Early Cretaceous TPW event formed a complete loop to provide solid evidence for the existence of fast TPW (see Hou et al.<sup>69</sup> and the references cited therein). Therefore, the paleolatitude evolution of Eurasia, Gondwana-India, and Gondwana-Australia are calculated from the fast TPW model based on Kent and Irving's model<sup>27</sup>. The paleolatitudes of Australia are calculated at a reference location (16°S, 113°E), and other paleolatitudes are calculated at a reference location (29.4°N, 88°E), cf. Supplementary Table 1<sup>9,13,14,18,20,23–26,42–49</sup>. An alternative scenario of subduction transference followed by ridge subduction soon afterwards, which requires the ridge to be close to the southern margin of Asia, is illustrated in Fig. 3. NQT North Qiangtang terrane, SQT South Qiangtang terrane, Lh Lhasa terrane. Other abbreviations (KX, NY, GD, etc.) indicate individual paleomagnetic results; refer to Supplementary Table 1 for full documentation.

In contrast, a paleolatitude difference of  $\sim 19.4^\circ$  ( $\sim 2200$  km) at 180 Ma between the expected paleolatitude of  $\sim 26^\circ$ S for eastern Gondwana (derived with Paleomagnetism.org) and the observed paleolatitude of  $\sim 6.6^\circ$ S for the Lhasa terrane reveals the extension of the Ceno-Tethys from  $\sim 219$  Ma to  $\sim 180$  Ma (Fig. 2A). Interpolating the Lhasa terrane paleolatitudes of  $\sim 17.0^\circ$ S at  $\sim 219$  Ma and  $\sim 6.6^\circ$ S at  $\sim 180$  Ma<sup>13,18</sup> yields a terrane motion of  $\sim 3.0$  cm/yr. The paleolatitude comparison between Lhasa and the northern margin of Australia during this period suggests that their separation most likely occurred at  $\sim 210$  Ma (Fig. 2A). Furthermore, the  $\sim 3.0$  cm/yr motion of the Lhasa terrane during the initial phase of its northward journey is significantly lower than its average motion of  $\sim 5.0$  cm/yr during  $\sim 219$ – $140$  Ma or  $\sim 4.5$  cm/yr during  $219$ – $130$  Ma, revealing a marked acceleration of the Lhasa terrane. Therefore, the breakup age of  $\sim 210$  Ma is deemed reliable. Pertaining to its uncertainty, uncertainties in paleolatitude and paleolatitude overlap are used to constrain its confidence interval. By this approach, the overlapping paleolatitudes within the confidence level indicate that their separation can be determined to no later than  $\sim 193$  Ma, reflecting a 17 Myr uncertainty for the minimum age. Paleolatitude overlap cannot define the maximum separation age, because tectonic units under consideration inherently overlap when juxtaposed, cf. Figure 2A. Therefore, we use here  $\sim 210$  Ma with an uncertainty of 17 Myr as the rifting age of the Lhasa terrane from Gondwana. Although this approach comes with a fairly moderate uncertainty interval, it provides the currently best possible paleolatitude evolution of the rifting, revealing that the Ceno-Tethys Ocean most likely opened at  $210 \pm 17$  Ma. A late Triassic break-up also fits well with the rift system between the Lhasa terrane and the northern margin of Gondwana, which became mature during the late Norian<sup>32</sup>, and with the Late Triassic (Norian/Rhaetian) to Late Jurassic (Oxfordian) extension in the Australian margin, which was accommodated in the upper crust by normal faulting and lower crustal thinning<sup>33</sup>.

Notably, the Sumdo eclogite and arc magmatic rocks within the Lhasa terrane suggest that the Lhasa terrane can be divided into a northern and southern subterrane separated by the Tangjia-Sumdo accretionary complex zone<sup>34</sup>. However, the evolution and scale of the Tangjia-Sumdo Ocean remain debated<sup>34–37</sup>. If that ocean existed, the Lhasa terrane likely had a more complex evolutionary history. The Ceno-Tethys Ocean and/or the Tangjia-Sumdo Ocean may have opened at or before the Permian<sup>35–37</sup>. The Lhasa terrane may have experienced two or possibly even more rifting events from the northern margin of Gondwana<sup>31,37,38</sup>. The northern Lhasa terrane rifted from the southern part at early Carboniferous times based on the Early Carboniferous meta-gabbro and metabasalt from the Tangjia-Sumdo area<sup>35</sup>. The southern Lhasa terrane rifted from the northern margin of Gondwana at the early to middle Permian based on the extension-type magmatism Permian Yawa intrusions in the southern Lhasa terrane<sup>39</sup> and the middle Permian composite seamount in the Yarlung Zangbo suture zone<sup>40</sup>. The breakup of the southern Lhasa terrane from Gondwana might have been followed by a Triassic collision and re-breakup<sup>38</sup>. This potential collision and re-breakup process can explain the apparent contradictory interpretations based on paleomagnetic<sup>13,20</sup> and magmatic<sup>35–37,41</sup> evidence.

Pertaining to the Late Triassic rifting event, the only reliable pre-Jurassic paleolatitude of  $17.0^\circ \pm 10.7^\circ$ S for the Lhasa terrane, obtained from the northern Lhasa subterrane<sup>20</sup>, indicates that the entire Lhasa terrane had become a coherent block by  $\sim 219$  Ma and was positioned close to the northern margin of Gondwana. A unified Lhasa terrane at this time is consistent with the closure of the Tangjia-Sumdo ocean at  $\sim 240$  Ma or earlier<sup>36,37</sup>. Therefore, we did not subdivide the Lhasa terrane in Figs. 2 and 3. Nevertheless, more reliable Permian–Triassic paleomagnetic data from the Lhasa terrane are needed to further constrain its drift history and the potential earlier opening and closing of both the Ceno-Tethys and Tangjia-Sumdo oceans.

### North Qiangtang–South Qiangtang collision at $\sim 220 \pm 15$ Ma

Marked differences in lithologic character and stratigraphy, magmatism, and fossil signatures indicate that the North Qiangtang terrane (NQT) and South Qiangtang terrane (SQT), separated by the Longmu Co-Shuanghu suture zone (LSSZ), have different drift histories<sup>9,42–48</sup> (Figs. 1, 2). The LSSZ represents the closure of a branch of the Paleo-Tethys Ocean due to the collision between SQT and NQT. Song et al.<sup>49</sup> and Yu et al.<sup>48</sup> determined a consistent paleolatitude of  $\sim 25^\circ$ N for the reference point (29.4°N, 88°E) in the Late Triassic ( $219 \pm 18$  Ma) for these terranes, forming the southern margin of Asia (Fig. 2A, H). In addition, the 230–209 Ma <sup>40</sup>Ar/<sup>39</sup>Ar age range of high-pressure to ultrahigh-pressure metamorphic rocks and the 225–205 Ma zircon U–Pb age range of magmatic rocks in the central part of the Qiangtang terrane, whose formation may have been triggered by slab breakoff after continental collision<sup>50</sup>, suggest that the SQT–NQT collision most likely occurred in the Late Triassic. The oldest continental sedimentary sequence of  $\sim 214$  Ma unconformably overlies an ophiolite mélange of  $\sim 220$  Ma in the Guoganzhian Mountain area, also pointing to a tectonic event at  $\sim 220$ – $214$  Ma at  $86^\circ$ E longitude<sup>51</sup>. The Paleo-Tethys Ocean likely closed at  $\sim 220$  Ma<sup>51</sup>. Therefore, the collision age is conservatively estimated at  $220 \pm 15$  Ma, with a relatively large uncertainty interval to include the age range of the magmatic flare-up and the exhumation of metamorphic rocks<sup>50</sup>.

### Lhasa–Qiangtang collision at $\sim 140 \pm 10$ Ma and India–Australia break up at $\sim 130 \pm 6$ Ma

The Jurassic–Cretaceous sedimentary, metamorphic, and magmatic records from the Lhasa–Qiangtang collision zone suggest that the collision most likely occurred at  $150$ – $130$  Ma<sup>52,53</sup>, which is supported by a consistent paleolatitude of Lhasa at  $\sim 130$  Ma and Qiangtang at  $\sim 150$  Ma ( $\sim 20^\circ$ N)<sup>26,54</sup>. Although reliable paleomagnetic data from  $\sim 140$  Ma are lacking, provenance analysis of the Cretaceous peripheral foreland basin sediments supports a Lhasa–Qiangtang collision at  $\sim 140$  Ma, quasi-simultaneously from east to west, which fits well with most of the geologic observations<sup>52</sup>. Therefore, the Lhasa–Qiangtang collision can be set at  $140 \pm 10$  Ma.

Marine magnetic anomaly data from the Perth Abyssal Plain, where the oceanic crust directly records the early spreading history between India and Australia, suggests that the initial breakup occurred at  $\sim 130$  Ma<sup>55</sup>. The

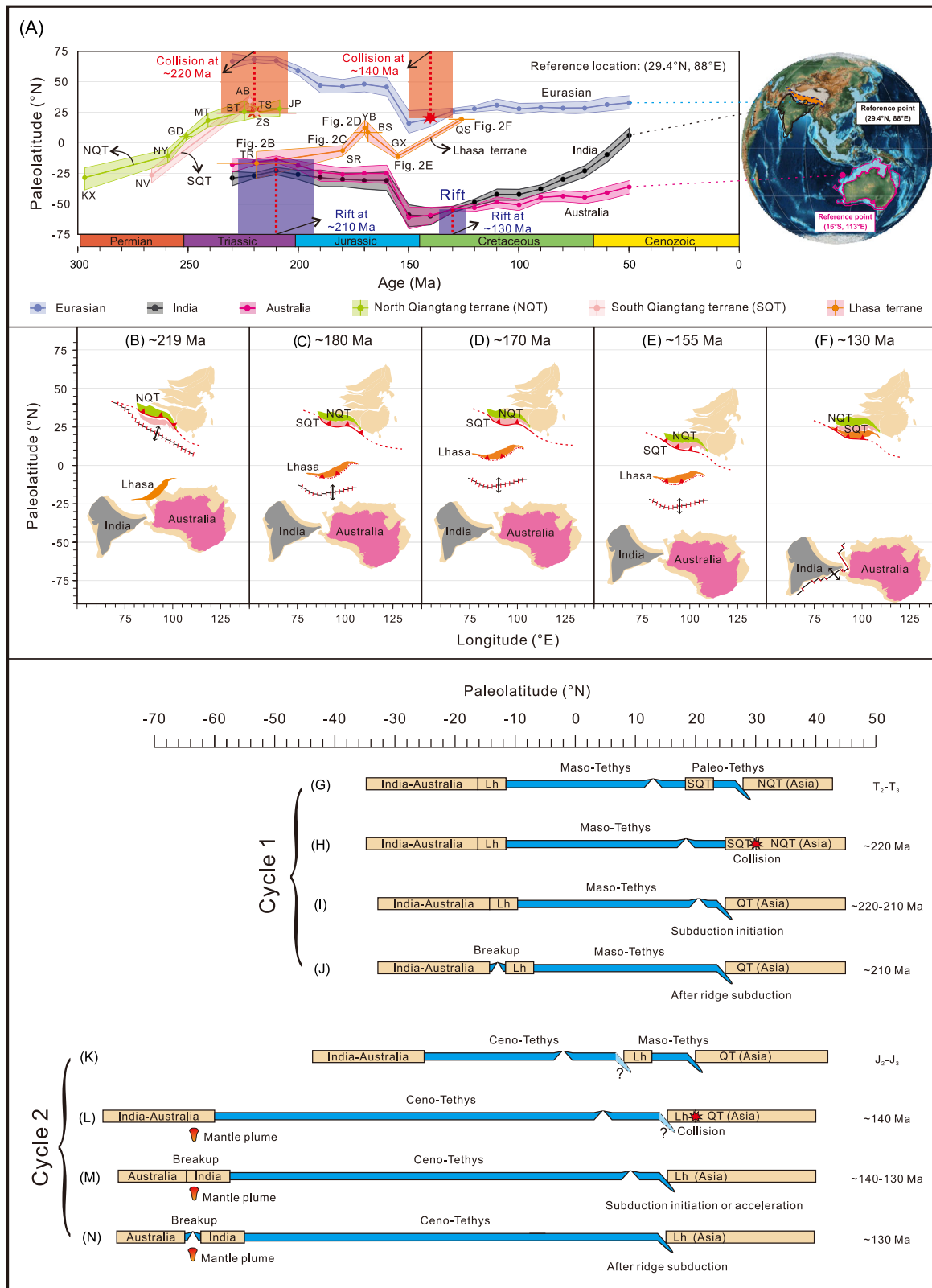


**Fig. 3 | Reconstruction of paleolatitude, paleogeography and kinematic cycles of the Lhasa terrane and adjacent blocks.** This figure shows the paleolatitude evolution (A) and paleo-position reconstruction (B-F) of the Lhasa terrane and adjacent blocks, including the two simplified kinematic cycles based on subduction transference followed by fast ridge subduction (G-N). Two subduction transference

events in cycle 1 (Fig. 3G-J) and cycle 2 (Fig. 3K-N) are identified in building Eurasia. The mid-ocean ridge of the Meso-Tethys Ocean and its subduction in the Late Triassic is reconstructed based on Scotese<sup>59</sup> (Fig. 3B, H, I), and that of the Ceno-Tethys Ocean in the Early Cretaceous is reconstructed based on Zhang et al.<sup>64</sup>. See also caption to Fig. 2.

temporal and spatial relationships between the Comei-Bunbury large igneous province and the Kerguelen mantle plume indicate that the Indian plate completely separated from the Australian-Antarctic plate before  $\sim 124$  Ma<sup>29</sup>. Therefore, an age of  $130 \pm 6$  Ma is used here to estimate the time of rifting of India from Australia-Antarctica.

### The spatiotemporal relationship between the collision and rifting events

Pertaining to the relationship between the SQT-NQT collision and the Gondwana-Lhasa rifting, a most likely age of  $\sim 220$  Ma for the collision fits well with subsequent arc magmatism in central Qiangtang that started at  $\sim 210$  Ma<sup>56,57</sup>, implying that the subduction initiation of the Meso-Tethys oceanic crust beneath the Qiangtang terrane occurred at  $\sim 220$ – $210$  Ma. The age gap between the continental collision and the subduction initiation is less than  $\sim 10$  Myr, which is consistent with numerical modeling results<sup>6</sup>. Our paleolatitude reconstruction points to an age of  $210 \pm 17$  Ma for the Gondwana-Lhasa rifting, i.e.,  $10 \pm 23$  Myr younger than the  $220 \pm 15$  Ma age of the SQT-NQT collision at the southern margin of Asia (Fig. 2A). The rifting of the Lhasa terrane from Gondwana is nearly coeval with the initiation of northward subduction of the Meso-Tethys. That is, the continental collision of the Qiangtang terrane and subsequent subduction transference seem to have a potential spatiotemporal relation with Lhasa's rifting from Gondwana. In addition, this age gap of  $\sim 10$  Myr is consistent with the time required for subduction initiation after a collision based on observations from the Qilian orogenic belt and numerical models<sup>5,6</sup>, implying that subduction transference may play a vital role in the one-way terrane convergence from Gondwana to Asia. This 10 Myr age interval is also consistent with the age interval documented for subduction reversal (similar to outboard jumping of the subduction zone, but with a change in the polarity of the slab) in several other orogens<sup>58</sup>.

For the relationship between the Lhasa-Qiangtang collision and the India-Australia rifting, a similar spatiotemporal relationship exists. There is an age gap of  $10 \pm 12$  Myr between the Lhasa-Qiangtang collision and the rifting of India. The similar spatiotemporal relationship between the collision and rifting events with similar age gaps of  $\sim 10$  Myr can be well explained by collision-induced subduction transference, which has been demonstrated by observation and numerical modeling. Next, we focus on whether ridge coupling is a required component in the scenario, explore alternatives, and discuss the first-order dynamics of the in-sequence northward convergence of the Tethys evolution.

### Coupling across the oceanic ridge/transform system model

The spatiotemporal relationship between the continental collision and the microcontinent rifting can be explained by collision-induced subduction transference. But how can the slab-pull force on the northern margin of Tethys fit with the rifting on its southern margin? Coupling (at least partial) must exist across the oceanic ridge/transform system within the ocean, so that the slab-pull force caused by collision-induced subduction transference in the north can be at least partly transmitted to the southern segment of the Meso- or Ceno-Tethys Ocean, triggering the rifting of Lhasa or India.

This effect (coupling across the oceanic ridge/transform system) should not be neglected and is supported by plate reconstructions. For example, the Pacific plate was bound to the north by spreading ridges but moved northward at high velocity during  $\sim 85$ – $55$  Ma<sup>59,60</sup>. Because the high velocity cannot be explained plausibly otherwise, the slab-pull force of the subducting Izanagi plate to the north of the ridge with (partial) coupling across the ridge/transform system should be invoked. In the Tethyan realm, since an oceanic ridge is typically offset by transform faults, the latter thus also connected the southern and northern parts of the Meso- or Ceno-Tethys. The geometry and orientation of the ridge/transform system in the Meso- and Ceno-Tethys oceans are not well determined, and different orientations of the ridge and transform segments would lead to different amounts of coupling. It has been suggested that the transform fault strength rheologically may be just slightly weaker than that of its surrounding

plates<sup>61</sup>, in particular under normal stresses, and the amount of coupling would also depend on the orientation of the ridge/transform system relative to the new subduction zone. The rheological strength of a transform fault/fracture zone system may thus be sufficient to transmit stress, due to (strong) coupling through the transform faults<sup>62,63</sup>, in particular, if these structures are at an angle about the tensional stresses induced by the slab-pull. Recent numerical models on trench-parallel oceanic ridge subduction also indicate that the transform fault and fracture zone should not be too weak for the lateral transmission of slab pull across the ridge<sup>63</sup>. Therefore, neighboring oceanic plates, separated by a ridge, are not totally decoupled<sup>63</sup>. Coupling across the ridge makes it possible for the slab-pull force to be transmitted, which is an important ingredient of the spatiotemporal relationship illustrated by our reconstruction. In this scenario, the cycles of the collision and rifting can be reconstructed as depicted in Fig. 2G–L (i.e., without having to invoke an early ridge subduction).

### Ridge subduction model

An alternative scenario for the observed spatiotemporal relationship may be ridge subduction soon after subduction transference, so that the slab-pull force can really be transmitted to the (originally) southern segment of the Meso- or Ceno-Tethys Ocean, triggering the rifting of Lhasa and India (Fig. 3).

The Eurasia-directed subduction of the oceanic spreading centers in the north of the Tethys Oceans may influence the fragmentation of Gondwana. In an ocean with an Andean-type subduction zone, it is straightforward to subduct ridges. This is because all the subduction must be accommodated by the trench-ward motion of the subducting (oceanic) plate. This is the case in the Pacific today and might have been even more pronounced in the Tethyan realm, where plate velocities  $>10$  cm/yr have been reported. Therefore, collision-induced subduction transference and ocean ridge subduction shortly after collision may be an alternative explanation for the spatiotemporal relationship.

Ridge subduction soon after subduction transference can also explain the age gap of  $\sim 10$  Myr between the SQT-NQT collision and the Gondwana-Lhasa rifting (Fig. 3G–J). After subduction transference, the ridge migrates towards the direction of most rapid subduction, especially in an ocean like the Tethys, which is bordered by a passive continental margin to the south and an active continental margin to the north<sup>8</sup>. This interpretation can also be supported by plate reconstructions. For example, Scotese<sup>59</sup> reconstructed the mid-ocean ridge of the Meso-Tethys close to the southern margin of Asia in the Late Triassic (Fig. 3B, H, I), supporting the fast subduction of the oceanic ridge below Asia scenario which enables the slab pull force being transferred to the passive margin of Gondwana which triggers the rifting of the Lhasa terrane (Fig. 3J).

For the age gap of  $\sim 10$  Myr between the Lhasa-Qiangtang collision and the rifting of India, the ridge is subducted shortly after the transference so that the slab-pull force can be transmitted to the southern edge of the Ceno-Tethys. In this scenario, the ridge is close to the southern margin of Asia (Fig. 3L, M). This scenario is also supported by plate reconstructions. Zhang et al.<sup>64</sup> suggest the ridge was close to the active continental margin during the Early Cretaceous based on paleomagnetic data of the Xigaze ophiolites in the Gangdese forearc<sup>65</sup>, supporting subduction of the northern segment of the Ceno-Tethys and the ridge at  $\sim 130$  Ma (Fig. 3M, N). After subduction of the ridge, the slab-pull-force was transferred from the Meso-Tethys to the southern segment of the Ceno-Tethys (Fig. 3K–N), dragging India to rift from Australia-Antarctica at  $130 \pm 6$  Ma.

In the scenario depicted in this section, the ridge should be close to the southern margin of Asia (Fig. 3). Given that the reconstruction of a ridge's position is subject to uncertainty, coupling (either full or partial) across the ridge/transform system may be a more likely scenario. In addition, the southward subduction model for the rifting of the Lhasa terrane is considered an option for potential debate on the existence and age of the southward subduction<sup>15,31,66</sup> (See Supplementary Note 1). Nevertheless, subduction transference is vital in all these models to explain the in-sequence one-way convergence of microcontinents with Asia.

## Dynamics of the in-sequence northward convergence

In summary, two similar geodynamic cycles are identified—both including the northward convergence of the Gondwana-derived terranes (Fig. 2G, J, and Fig. 3G, K), their collision with Asia (Fig. 2H, K, Fig. 3H, L), collision-induced subduction initiation [(or acceleration) see Supplementary Note 2] of the younger Tethys slab (Fig. 2I, L, and Fig. 3I, M) and the breakup of the next terrane from Gondwana (Fig. 2I, L) [after a fast ridge subduction (Fig. 3J, N)].

The evolution of an ocean basin from opening to closing is referred to as a Wilson cycle. The opening to the closing cycle of the Paleo-, Meso-, and Ceno-Tethys Oceans thus correspond to three successive “Wilson cycles”. The Paleo-Tethys here only refers to a branch of the Paleo-Tethys (Longmu Co-Shuanghu Ocean) that opened between the NQT and SQT based on their different drift histories, but it does not refer to another branch of the Paleo-Tethys (Jinshajiang Ocean) between the Qiangtang terrane and the Tarim-Qaidam Blocks. Given the same age gap of ~10 Myr for the “collision-subduction transference-rift” process, we refer to these processes that linked three successive Wilson cycles as “Linked-Wilson cycles” (Fig. 2). The dynamics of each Linked-Wilson cycle can be summarized as follows. Before each terrane collision, the respective oceanic plates continued to be subducted beneath Asia due to the slab-pull force, pulling the microcontinent northward. When a positively buoyant terrane (or microcontinent) collides with the southern margin of Asia, an active continental margin, the subduction zone to the north of the accreted terrane becomes clogged because the positively buoyant continental lithosphere has difficulty continuing subduction like the oceanic lithosphere<sup>5</sup>. After the continental collision, however, the Tethyan oceanic crust to the south of the collided terrane continued to move northward after the subduction zone stepped out to the outboard side of the accreted terrane. In this process, stress concentration occurred at the junction between the Tethyan Ocean and the new southern margin of Asia, positioning the junction ideally for potential subduction initiation<sup>6,67</sup>. The slab-pull force caused by subduction transference can be transmitted to the northern margin of Gondwana through coupling across the ridge/transform system, triggering rifting and the northward motion of microcontinents from Gondwana to Asia. Subduction of the ridge eventually facilitates the northward drift of the microcontinents.

The similar spatiotemporal relationship revealed by the Linked-Wilson cycles suggests that subduction transference and/or acceleration plays a vital role in the one-way convergence from Gondwana to Asia, at least for the Tibetan realm. The fate of the Wilson cycle of the respective terranes was probably sealed before it even began.

## Data availability

All study data are included in the article and/or supporting information, including Supplementary Notes 1 and 2 and Supplementary Table 1. These data can be download at files section at <https://doi.org/10.17605/OSF.IO/RN3FA>.

Received: 12 February 2025; Accepted: 22 May 2025;

Published online: 06 June 2025

## References

- Conrad, C. P. & Lithgow-Bertelloni, C. How mantle slabs drive plate tectonics. *Science* **298**, 207–209 (2002).
- Frisch, W. Meschede, M. & Blakey, R. *Plate Tectonics: Continental Drift and Mountain Building* (Springer, 2011).
- Wan, B. et al. Cyclical one-way continental rupture-drift in the Tethyan evolution: subduction-driven plate tectonics. *Sci. China Earth Sci.* **62**, 2005–2016 (2019).
- Zhu, R. X., Zhao, P., Wan, B. & Sun, W. D. Geodynamics of the one-way subduction of the Neo-Tethys Ocean. *Chin. Sci. Bull. Chin.* **68**, 1699–1708 (2023).
- Yang, G. Subduction initiation triggered by collision: a review based on examples and models. *Earth-Sci. Rev.* **232**, 104129 (2022).
- Zhong, X. & Li, Z.-H. Subduction initiation during collision-induced subduction transference: numerical modeling and implications for the tethyan evolution. *J. Geophys. Res.-Solid Earth* **125**, e2019JB019288 (2020).
- Metcalfe, I. Multiple Tethyan ocean basins and orogenic belts in Asia. *Gondwana Res.* **100**, 87–130 (2021).
- Yin, A. Geologic evolution of the Himalayan-Tibetan orogen—growth of the Asian continent in the Phanerozoic. *Acta Geosci. Sin.* **22**, 193–230 (2001).
- Song, P. P. et al. Late Triassic paleolatitude of the Qiangtang block: implications for the closure of the Paleo-Tethys Ocean. *Earth Planet. Sci. Lett.* **424**, 69–83 (2015).
- Ma, Y. M. et al. A stable Southern margin of Asia during the cretaceous: paleomagnetic constraints on the Lhasa-Qiangtang collision and the maximum width of the Neo-Tethys. *Tectonics* **37**, 3853–3876 (2018).
- Jin, S. et al. A smaller greater India and a middle-early eocene collision with Asia. *Geophys. Res. Lett.* **50**, e2022GL101372 (2023).
- Allegre, C. J. et al. Structure and evolution of the Himalaya-Tibet orogenic belt. *Nature* **307**, 17–22 (1984).
- Li, Z. Y. et al. Paleomagnetic constraints on the Mesozoic drift of the Lhasa terrane (Tibet) from Gondwana to Eurasia. *Geology* **44**, 727–730 (2016).
- Ran, B. et al. New paleomagnetic results of the early Permian in the Xainza area, Tibetan Plateau and their paleogeographical implications. *Gondwana Res.* **22**, 447–460 (2012).
- Şengör, A. M. C. et al. On the nature of the Cimmerian Continent. *Earth-Sci. Rev.* **247**, 104520 (2023).
- Stampfli, G. M. & Borel, G. D. A plate tectonic model for the Paleozoic and Mesozoic constrained by dynamic plate boundaries and restored synthetic oceanic isochrons. *Earth Planet. Sci. Lett.* **196**, 17–33 (2002).
- Zhu, D. C., Zhao, Z. D., Niu, Y. L., Dilek, Y. & Mo, X. X. Lhasa terrane in southern Tibet came from Australia. *Geology* **39**, 727–730 (2011).
- Ma, Y. M. et al. Jurassic paleomagnetism of the Lhasa Terrane—implications for Tethys evolution and true polar wander. *J. Geophys. Res. Solid Earth* **127**, e2022JB025577 (2022).
- Torsvik, T. H. et al. Phanerozoic polar wander, palaeogeography and dynamics. *Earth Sci. Rev.* **114**, 325–368 (2012).
- Zhou, Y. N. et al. Paleomagnetic study on the Triassic rocks from the Lhasa Terrane, Tibet, and its paleogeographic implications. *J. Asian Earth Sci.* **121**, 108–119 (2016).
- Van der Voo, R. The reliability of paleomagnetic data. *Tectonophysics* **184**, 1–9 (1990).
- Meert, J. G. et al. The magnificent seven: a proposal for modest revision of the Van der Voo (1990) quality index. *Tectonophysics* **790**, 228549 (2020).
- Li, Z. Y. et al. Jurassic true polar wander recorded by the Lhasa terrane on its northward journey from Gondwana to Eurasia. *Earth Planet. Sci. Lett.* **592**, 117609 (2022).
- Otofuiji, Y. I. et al. Spatial gap between Lhasa and Qiangtang blocks inferred from Middle Jurassic to Cretaceous paleomagnetic data. *Earth Planet. Sci. Lett.* **262**, 581–593 (2007).
- Wang, S. et al. New Middle Jurassic Paleomagnetic and Geochronologic Results From the Lhasa Terrane: Contributions to the Closure of the Meso-Tethys Ocean and Jurassic True Polar Wander. *Geophys. Res. Lett.* **50**, e2023GL103343 (2023).
- Ma, Y. et al. Paleomagnetism and U-Pb zircon geochronology of Lower Cretaceous lava flows from the western Lhasa terrane: New constraints on the India-Asia collision process and intracontinental deformation within Asia. *J. Geophys. Res.-Solid Earth* **119**, 7404–7424 (2014).
- Kent, D. V. & Irving, E. Influence of inclination error in sedimentary rocks on the Triassic and Jurassic apparent pole wander path for

- North America and implications for Cordilleran tectonics. *J. Geophys. Res. Solid Earth* **115**, B10103 (2010).
28. Koymans, M. R., Langereis, C. G., Pastor-Galan, D. & van Hinsbergen, D. J. J. Paleomagnetism.org: An online multi-platform open source environment for paleomagnetic data analysis. *Comput. Geosci.* **93**, 127–137 (2016).
29. Bian, W. W. et al. Paleomagnetic and Geochronological Results From the Zhela and Weimei Formations Lava Flows of the Eastern Tethyan Himalaya: New Insights Into the Breakup of Eastern Gondwana. *J. Geophys. Res. Solid Earth* **124**, 44–64 (2019).
30. Wang, Q., Zhu, D. C., Cawood, P. A., Chung, S. L. & Zhao, Z. D. Resolving the Paleogeographic Puzzle of the Lhasa Terrane in Southern Tibet. *Geophys. Res. Lett.* **48**, e2021GL094236 (2021).
31. Zhu, D.-C. et al. The origin and pre-Cenozoic evolution of the Tibetan Plateau. *Gondwana Res.* **23**, 1429–1454 (2013).
32. Liu, G. & Einsele, G. Sedimentary history of the Tethyan basin in the Tibetan Himalayas. *Geol. Rundsch.* **83**, 32–61 (1994).
33. Advokaat, E. L. & van Hinsbergen, D. J. J. Finding Argoland: reconstructing a microcontinental archipelago from the SE Asian accretionary orogen. *Gondwana Res.* **128**, 161–263 (2024).
34. Yang, J. et al. Discovery of an eclogite belt in the Lhasa block, Tibet: a new border for Paleo-Tethys?. *J. Asian Earth Sci.* **34**, 76–89 (2009).
35. Wang, B. et al. Opening of the Sumdo Paleo-Tethys Ocean and rifting of the Lhasa terrane from Gondwana: insights from early Carboniferous magmatism in southern Tibet. *GSA Bull.* **136**, 531–546 (2023).
36. Wang, X., Lang, X., Klemd, R., Deng, Y. & Tang, J. Subduction initiation of the Neo-Tethys oceanic lithosphere by collision-induced subduction transference. *Gondwana Res.* **104**, 54–69 (2022).
37. Wang, X. et al. Early carboniferous back-arc rifting-related magmatism in Southern Tibet: implications for the history of the Lhasa Terrane separation From Gondwana. *Tectonics* **39**, e2020TC006237 (2020).
38. Qayyum, A. et al. Subduction and slab detachment under moving trenches during ongoing India-Asia convergence. *Geochem. Geophys. Res. Lett.* **23**, e2022GC010336 (2022).
39. Zeng, Y.-C. et al. Initial Rifting of the Lhasa Terrane from Gondwana: insights from the Permian (similar to 262Ma) amphibole-rich lithospheric mantle-derived Yawa Basanitic intrusions in Southern Tibet. *J. Geophys. Res. Solid Earth* **124**, 2564–2581 (2019).
40. Fan, X. et al. Lithofacies, geochemistry, and sequences of basalt and carbonate rocks of a Middle Permian composite seamount (central Yarlung Zangbo Suture Zone, Tibet): Implications to the incipient opening of the Neo-Tethys Ocean. *Lithos* **448–449**, 107175 (2023).
41. Wang, C. et al. Petrogenesis of Middle-Late Triassic volcanic rocks from the Gangdese belt, southern Lhasa terrane: implications for early subduction of Neo-Tethyan oceanic lithosphere. *Lithos* **262**, 320–333 (2016).
42. Guan, C. et al. Paleomagnetic and Chronologic Data Bearing on the Permian/Triassic Boundary Position of Qamdo in the Eastern Qiantang Terrane: Implications for the closure of the Paleo-Tethys. *Geophys. Res. Lett.* **48**, e2020GL092059 (2021).
43. Ma, Y. M. et al. Paleomagnetic constraints on the origin and drift history of the North Qiantang Terrane in the Late Paleozoic. *Geophys. Res. Lett.* **46**, 689–697 (2019).
44. Song, P. P., Ding, L., Li, Z. Y., Lippert, P. C. & Yue, Y. H. An early bird from Gondwana: paleomagnetism of Lower Permian lavas from northern Qiantang (Tibet) and the geography of the Paleo-Tethys. *Earth Planet. Sci. Lett.* **475**, 119–133 (2017).
45. Song, P. P. et al. Paleomagnetism of middle Triassic Lavas from Northern Qiantang (Tibet): constraints on the closure Of the Paleo-Tethys Ocean. *J. Geophys. Res. Solid Earth* **125**, e2019JB017804 (2020).
46. Wei, B. et al. Placing another piece of the Tethyan Puzzle: the first paleozoic paleomagnetic data from the South Qiantang Block and its paleogeographic implications. *Tectonics* **41**, e2022TC007355 (2022).
47. Wei, B. et al. Paleomagnetism of late triassic volcanic rocks from the South Qiantang Block, Tibet: constraints on Longmuco-Shuanghu Ocean closure in the paleo-tethys realm. *Geophys. Res. Lett.* **50**, e2023GL104759 (2023).
48. Yu, L. et al. New paleomagnetic and chronological constraints on the late triassic position of the Eastern Qiantang Terrane: implications for the closure of the Paleo-Jinshajiang Ocean. *Geophys. Res. Lett.* **49**, e2021GL096902 (2022).
49. Song, C. et al. Late Triassic paleomagnetic data from the Qiantang Terrane of Tibetan plateau and their Tectonic significances. *J. Jilin Univ. Earth Sci. Ed.* **42**, 526–535 (2012).
50. Wu, H., Li, C., Chen, J. & Xie, C. Late Triassic tectonic framework and evolution of Central Qiantang, Tibet, SW China. *Lithosphere* **8**, 141–149 (2016).
51. Li, C., Zhai, Q., Dong, Y., Yu, J. & Huang, X. Establishment of the upper triassic Wanghuling formation at Guoganjianian Mountain, Central Qiantang, Qinghai-Tibet Plateau, and its significance. *Geol. Bull. China* **26**, 1003–1008 (2007).
52. Chen, Y. et al. Provenance analysis of Cretaceous peripheral foreland basin in central Tibet: Implications to precise timing on the initial Lhasa-Qiantang collision. *Tectonophysics* **775**, 228311 (2020).
53. Li, S., Yin, C. Q., Guilmette, C., Ding, L. & Zhang, J. Birth and demise of the Bangong-Nujiang Tethyan Ocean: A review from the Gerze area of central Tibet. *Earth Sci. Rev.* **198**, 102907 (2019).
54. Yan, M. et al. Paleomagnetic data bearing on the Mesozoic deformation of the Qiantang Block: implications for the evolution of the Paleo- and Meso-Tethys. *Gondwana Res.* **39**, 292–316 (2016).
55. Williams, S. E., Whittaker, J. M., Granot, R. & Müller, D. R. Early India-Australia spreading history revealed by newly detected Mesozoic magnetic anomalies in the Perth Abyssal Plain. *J. Geophys. Res. Solid Earth* **118**, 3275–3284 (2013).
56. Liu, Y. et al. Jurassic tectonic evolution of Tibetan Plateau: a review of Bangong-Nujiang Meso-Tethys Ocean. *Earth-Sci. Rev.* **227**, 103973 (2022).
57. Zeng, M. et al. Late Triassic initial subduction of the Bangong-Nujiang Ocean beneath Qiantang revealed: stratigraphic and geochronological evidence from Gaize, Tibet. *Basin Res.* **28**, 147–157 (2016).
58. Brown D., et al. *Arc-Continent Collision: The Making of an Orogen* (Springer, 2011).
59. Scotese C. Plate tectonic evolution during the last 1.5 billion years: the movie. Geological Society of America Annual Meeting in Indianapolis, Indiana, USA (2018).
60. Doubrovine, P. V., Steinberger, B. & Torsvik, T. H. Absolute plate motions in a reference frame defined by moving hot spots in the Pacific, Atlantic, and Indian oceans. *J. Geophys. Res. Solid Earth* **117**, B09101 (2012).
61. Maia M. Chapter 3 - Topographic and morphologic evidences of deformation at oceanic transform faults: far-field and local-field stresses. In: *Transform Plate Boundaries and Fracture Zones* (ed Duarte J. C.). (Elsevier, 2019).
62. Croon, M. B., Cande, S. C. & Stock, J. M. Abyssal hill deflections at Pacific-Antarctic ridge-transform intersections. *Geochem. Geophys. Res. Lett.* **11**, Q11004 (2010).
63. Cui, Q. & Li, Z.-H. Trench-parallel mid-ocean ridge subduction driven by along-strike transmission of slab pull. *Geology* **52**, 943–947 (2024).
64. Zhang, C. et al. Subduction re-initiation at dying ridge of Neo-Tethys: insights from mafic and metamafic rocks in Lhaze ophiolitic mélange, Yarlung-Tsangbo Suture Zone. *Earth Planet. Sci. Lett.* **523**, 115707 (2019).
65. Huang, W. et al. Lower Cretaceous Xigaze ophiolites formed in the Gangdese forearc: evidence from paleomagnetism, sediment

- provenance, and stratigraphy. *Earth Planet. Sci. Lett.* **415**, 142–153 (2015).
66. Kapp, P. & DeCelles, P. G. Mesozoic–Cenozoic geological evolution of the Himalayan–Tibetan orogen and working tectonic hypotheses. *Am. J. Sci.* **319**, 159–254 (2019).
67. Zhou, X., Li, Z.-H., Gerya, T. V. & Stern, R. J. Lateral propagation–induced subduction initiation at passive continental margins controlled by preexisting lithospheric weakness. *Sci. Adv.* **6**, eaaz1048 (2020).
68. Fu, R. R. & Kent, D. V. Anomalous Late Jurassic motion of the Pacific Plate with implications for true polar wander. *Earth Planet. Sci. Lett.* **490**, 20–30 (2018).
69. Hou, Y. et al. Completing the loop of the Late Jurassic–Early Cretaceous true polar wander event. *Nat. Commun.* **15**, 2183 (2024).

## Acknowledgements

We appreciate the helpful suggestions of associate editor Carolina Ortiz Guerrero, Prof. John Geissman and an anonymous reviewer. We also thank Prof. Douwe J. J. van Hinsbergen for helpful discussions and suggestions regarding coupling at oceanic ridges. This study was supported by National Natural Science Foundation of China (grant nos. 42174089) and the Knowledge Innovation Program of Wuhan–Shuguang 2023020201020338. J.C.D. is supported by an FCT contract CEEC Inst. 2018, CEECINST/00032/2018/CP1523/CT0002. This work was also supported by the Portuguese Fundação para a Ciência e Tecnologia, FCT, I.P./MCTES through national funds (PIDDAC): UID/50019/2025 and LA/P/0068/2020 (<https://doi.org/10.54499/LA/P/0068/2020>).

## Author contributions

Y.M., M.J.D., J.D., and T.K. wrote the paper.

## Competing interests

The authors declare that they have no competing interests. João C. Duarte is an Editorial Board Member for *Communications Earth & Environment*, but was not involved in the editorial review of, nor the decision to publish this article.

## Additional information

**Supplementary information** The online version contains supplementary material available at <https://doi.org/10.1038/s43247-025-02410-1>.

**Correspondence** and requests for materials should be addressed to Yiming Ma.

**Peer review information** *Communications Earth & Environment* thanks John W. Geissman and the other, anonymous, reviewer(s) for their contribution to the peer review of this work. Primary Handling Editors: Carolina Ortiz Guerrero [A peer review file is available].

**Reprints and permissions information** is available at <http://www.nature.com/reprints>

**Publisher's note** Springer Nature remains neutral with regard to jurisdictional claims in published maps and institutional affiliations.

**Open Access** This article is licensed under a Creative Commons Attribution-NonCommercial-NoDerivatives 4.0 International License, which permits any non-commercial use, sharing, distribution and reproduction in any medium or format, as long as you give appropriate credit to the original author(s) and the source, provide a link to the Creative Commons licence, and indicate if you modified the licensed material. You do not have permission under this licence to share adapted material derived from this article or parts of it. The images or other third party material in this article are included in the article's Creative Commons licence, unless indicated otherwise in a credit line to the material. If material is not included in the article's Creative Commons licence and your intended use is not permitted by statutory regulation or exceeds the permitted use, you will need to obtain permission directly from the copyright holder. To view a copy of this licence, visit <http://creativecommons.org/licenses/by-nc-nd/4.0/>.

© The Author(s) 2025